Biological uptake, water mass mixing and scavenging prevent transport of manganese-rich waters from the Antarctic shelf

P. Latour[1,2*], P. van der Merwe[1,2], K. Wuttig[2], M. Corkill[1], A. T. Townsend[3], T. M. Holmes[4], S. R. Rintoul[4-6], R. Schlitzer[7], C. Weldrick[4], R. F. Strzepek[2,4], M. Gault-Ringold[2] and A. R. Bowie[1,2]

[1]Institute for Marine and Antarctic Studies, University of Tasmania, Locked Bag 129, Hobart, TAS 7001, Australia

[2]Antarctic Climate and Ecosystems Cooperative Research Centre (ACE CRC), University of Tasmania, Private Bag 80, Hobart, TAS 7001, Australia

[3]Central Science Laboratory (CSL), University of Tasmania, Private Bag 74, Hobart, TAS 7001, Australia

[4]Australian Antarctic Program Partnership (AAPP), Institute for Marine and Antarctic Studies, University of Tasmania, Hobart, TAS, 7001, Australia

[5]CSIRO Oceans & Atmosphere, Hobart, TAS, Australia

[6]Centre for Southern Hemisphere Oceans Research, Hobart, TAS, Australia

[7]Alfred Wegener Institute for Polar and Marine Research, Postfach 120161, 27515 Bremerhaven, Germany

Corresponding author: Pauline Latour (pauline.latour@utas.edu.au)

Key Points:

- High dissolved manganese concentrations observed over the East Antarctic shelf, decreasing with distance from the coast
- Biological uptake decreases Mn export in surface waters
- Dilution of Mn-rich Antarctic Bottom Waters with Mn-depleted Low Circumpolar Deep Waters and scavenging processes decrease Mn export in bottom waters

Abstract

Manganese (Mn) is an essential element for photosynthetic life, yet concentrations in Southern Ocean open waters are very low, resulting from biological uptake along with limited external inputs. At southern latitudes, waters overlying the Antarctic shelf are expected to have much higher Mn concentrations due to their proximity to external sources such as sediment and sea ice. In this study, we investigated the potential export of Mn-rich Antarctic shelf waters toward depleted open Southern Ocean waters. Our results showed that while high Mn concentrations were observed over the shelf, strong biological uptake decreased dissolved Mn concentrations in surface waters north of the Southern Antarctic Circumpolar Current Front (< 0.1 nM), limiting export of shelf Mn to the open Southern Ocean. Conversely, in bottom waters, mixing between Mn-rich Antarctic Bottom Waters and Mn-depleted Low Circumpolar Deep Waters combined with scavenging processes led to a decrease in dissolved Mn concentrations with distance from the coast. Subsurface dissolved Mn maxima represented a potential reservoir for surface waters (0.3 – 0.6 nM). However, these high subsurface values decreased with distance from the coast, suggesting these features may result from external sources near the shelf in addition to particle remineralization. Overall, these results imply that the lower-than-expected lateral export of trace

metal-enriched waters contributes to the extremely low (< 0.1 nM) and potentially co-limiting Mn concentrations previously reported further north in this Southern Ocean region.

1. Introduction

Manganese (Mn) is a key bioactive trace metal essential for the growth of phytoplankton in the ocean (Armstrong 2008; Middag et al. 2011). It is required for the oxygen evolving complex that produces electrons for photosynthesis (Armstrong 2008), and is also involved in the defence against reactive oxygen species (Peers and Price 2004). Despite being the 12th most abundant element in the Earth's crust (Wedepohl, 1995), Mn is found at very low concentrations in seawater, typically in the nanomolar range (Klinkhammer and Bender, 1980; Westerlund and Öhman 1991; Middag et al. 2013; Browning et al. 2014). These low concentrations can lead to Mn (co-)limitation of phytoplankton growth, especially in High-Nutrient Low-Chlorophyll (HNLC) regions such as the Southern Ocean where phytoplankton growth is already iron (Fe) limited (Wu et al. 2019; Browning et al. 2021). This limitation directly impacts the carbon cycle through modification of the strength of the ocean's biological carbon pump (Boyd et al. 2000). Knowing the distribution, sources, sinks and cycling of bioactive trace metals such as Mn remains essential to predict future changes in the marine carbon cycle using biogeochemical models.

In seawater, the Mn distribution is controlled by its complex redox cycle and external sources/sinks. Manganese is often studied by separating its dissolved (dMn) and particulate (pMn) phases, typically via 0.2 µm filtration (Cutter et al. 2017). The dissolved phase is expected to be composed of the most reduced Mn species (Mn(II)) while pMn is primarily composed of Mn oxides (Sunda and Huntsman 1988; Twining et al. 2015) but can also include Mn within phytoplankton or minerals (Sunda and Huntsman 1994). Multiple external sources have been identified to supply dissolved and particulate Mn to seawater such as sediment resuspension (Middag et al. 2011; Cheize et al. 2019), hydrothermal vents (Resing et al. 2015; Holmes et al., 2017), atmospheric deposition (Xu and Gao 2014), riverine outflow (Aguilar-Islas and Bruland 2006), glacial discharge (Bhatia et al. 2021) and sea ice melting (Grotti et al. 2005). In addition, redox mobilization from sediments, associated with diagenetic processes and bacterial degradation of organic matter, has been described as a strong source of dMn (Sundby et al. 1986). Yet, these complex processes near the sediment/water interface are tightly linked to oxygen concentrations and can either increase or remove dMn through Mn oxides dissolution or dMn precipitation, respectively (Sundby et al. 1986). Overall, sediments are usually identified as Mn sources, associated with Mn-enriched subsurface plumes often observed along coastlines (Oldham et al. 2017; Morton et al. 2019).

In the Southern Ocean, dMn concentrations are controlled by biological uptake in the surface layer, remineralization below the photic zone, scavenging at greater depths and external inputs near the seafloor (Middag et al. 2011; 2013). The pMn fraction has rarely been studied in open waters of the Southern Ocean (Bowie et al. 2009; 2010; van der Merwe et al. 2019; Latour et al. 2021) and the distribution between labile and refractory pools even less so. From studies to date, the total particulate fraction is characterised by very low surface concentrations, increasing with depth with a marked increase near the seafloor. A small excess of labile pMn relative to refractory fractions was noted in samples collected from the Australian sector of the Southern Ocean (51-63%; Latour et al. 2021). The labile particulate fraction is expected to be more bioavailable for phytoplankton uptake, while the refractory fraction is thought to be inaccessible (Berger et al. 2008). Overall, low Southern Ocean trace metal concentrations have been

attributed to the oceanic isolation of the Antarctic continent by the Antarctic Circumpolar Current (ACC) and to low atmospheric inputs due to the vast distance from ice-free land masses (Wagener et al. 2008).

At higher latitudes, Antarctica represents a source of lithogenic material, yet studies documenting the lateral export of trace metals in lithogenic material remain scarce (Measures et al. 2013). In particular, very few studies have described the dissolved and particulate trace metal concentrations in seawater off the Adélie and George V Lands, in East Antarctica, with most studies focusing on sea ice concentrations (Lannuzel et al. 2011; 2014; Duprat et al. 2020). Smith et al. (2021) presented the first seawater concentrations of dMn in the Mertz Glacier region with relatively high dMn concentrations observed over the shelf (> 0.4 nM), attributed to sediment inputs. Dissolved and particulate Mn concentrations have also been reported in the Ross Sea, ranging from 0.34 to 0.78 nM and 0.01 to 0.51 nM, respectively (Fitzwater et al. 2000; Corami et al. 2005). However, spatial variability between coastal Antarctic regions are expected (Angino 1966), necessitating further studies.

The continental shelf adjacent to Adélie and George V land is characterised by several banks and depressions influencing regional oceanic circulation (Rintoul 1998; Beaman et al. 2011). This area also includes the Mertz polynya, which is a region of high sea ice production and bottom water formation (Rintoul 1998), as well as high primary productivity (Liniger et al. 2020). As Antarctic coastal areas represent important ecological hot spots and efficient carbon sinks (Arrigo et al. 2015), identifying trace metal distributions in these regions is vital for understanding the bottom-up control of biological carbon assimilation. In addition, high concentrations of Mn and other trace metals derived from lithogenic sources on the Antarctic shelf may be exported to the open Southern Ocean by northward transport of surface waters or the formation and export of bottom waters. In this study, we present dissolved and particulate Mn concentrations along three latitudinal transects in the Adélie and George V Lands region (with a zonal section along ~62°S joining them), in addition to three stations located on the periphery of the Adélie Bank. These results are interpreted using ratios with the lithogenic tracer titanium (Ti) and macronutrients as indicators of biological activity. Specifically, we investigated the northward transport of heavily Mn-enriched waters from the East Antarctic coast toward open waters of the Southern Ocean. Distributions of Fe and other bioessential trace metals will be presented in a later companion paper.

2. Materials and Methods

2.1 Sampling area

Multiple stations were sampled off the East Antarctic coast during the GEOTRACES GS01 voyage (IN2018-V01) in austral summer 2018 onboard RV Investigator, between 62°S-66.4°S and 132°E-150°E (Figure 1). Samples were collected along three latitudinal transects, located at 132°E, 140°E and 150°E, hereafter referred to as 132, 140 and 150, respectively. The Mn distribution along 140, which is the southern end of the GEOTRACES-SR3 transect, has previously been reported by Latour et al. (2021). The three transects were joined by the zonal S4 section (~62-64°S). Additionally, three stations were sampled on the edge of the Adélie Bank.

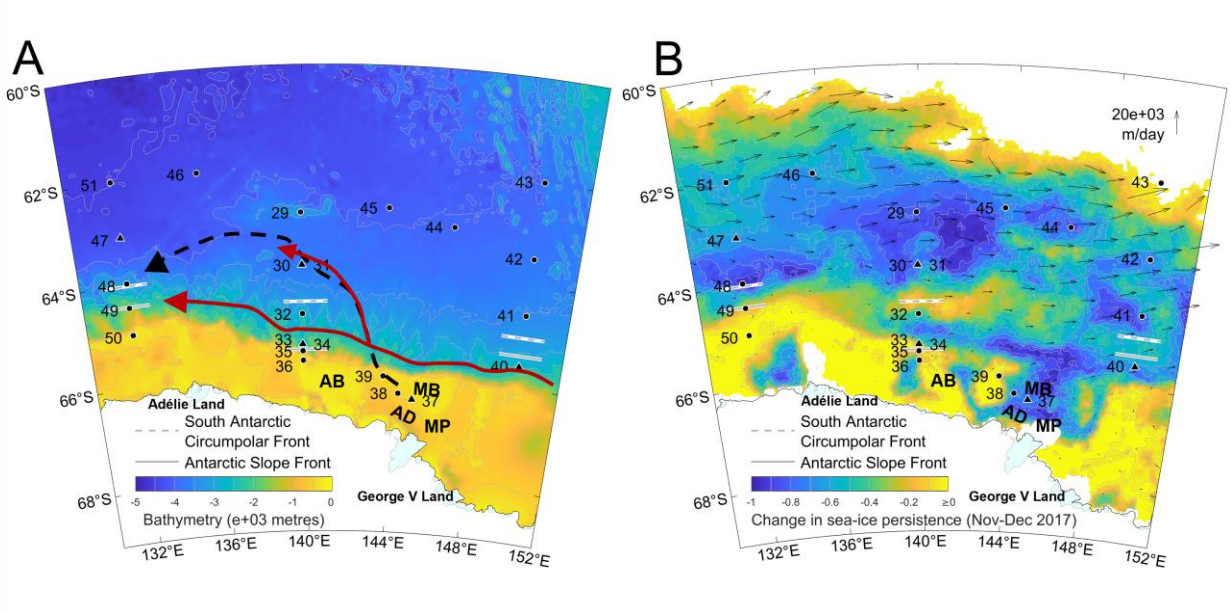

Figure 1: Map of the study area showing the bathymetry background colour overlaid with trace metal rosette station locations (black dots) (A). Triangles show stations where in-situ pumps were deployed. The large arrows indicate bottom water flow in this region for Ross Sea Bottom Water (RSBW, in red) and Adélie Land Bottom Water (ALBW, dashed black) from Foppert et al. (2021). On the right panel (B), the colour shows the change in sea ice persistence between November and December 2017, prior to our occupation (Spreen et al., 2008). Values ≥ 0 indicate no change in the proportion of sea ice occurred between November and December while a value of -1 indicate that where sea ice was present for all of November, it was absent for all of December. Overlaid small black arrows represent the average sea ice velocity for November and December (Kimura et al., 2004). The South Antarctic Circumpolar Front and the Antarctic Slope Front are indicated by dashed and solid grey lines on each panel. The location of the Adélie Bank (AB), Adélie Depression (AD), Mertz Bank (MB) and Mertz Polynya (MP) are indicated on both panels.

The hydrology of the region was studied through multiple deployments of a 36-bottle Conductivity-Temperature-Depth (CTD) rosette, also measuring oxygen, fluorescence, photosynthetic active radiation (PAR) and transmittance (Sea-Bird Electronics sensors: SBE4C, SBE3T, SBE9plus, SBE43, FLBBNTU, QCP – 2300 HP and Wetlabs CSTAR 25cm). Temperature and salinity measurements were used to identify water masses. The combination of fluorescence, PAR and transmittance was used to locate higher biomass and identify non-photochemical quenching (NPQ; Horton et al. 1996). This phenomenon occurs when phytoplankton are exposed to high light intensities and divert energy through heat rather than fluorescence. In this case, fluorescence sensors can display a ‘false deep chlorophyll maximum’. By combining fluorescence, PAR and transmittance, these ‘false deep chlorophyll maxima’ can be easily identified with transmittance, confirming the presence of particles (likely phytoplankton) in the top layer.

Stations in Figure 1 were sampled for dissolved trace metal concentrations using a trace metal rosette (TMR). Five stations were studied for particulate trace metal concentrations through deployments of in-situ pumps (ISPs) (triangles in Figure 1) (McLane Research Laboratories, WTS_LV). A chemical leach following the method of Berger et al. (2008) of ISP samples in the laboratory yielded both labile and refractory particulate fractions. Discrete (4L) samples for total particulate trace metal concentrations were also collected from the TMR to compliment the ISP sampling and expand the spatial resolution of particulate trace metal data. Samples for dissolved

macronutrient concentrations were collected at each CTD cast, and analysed onboard using segmented flow analyses (Rees et al. 2018).

2.2 Trace metal sample processing and analysis

The processing of both dissolved and particulate trace metal samples followed GEOTRACES recommendations (Cutter et al. 2017). A detailed method for equipment preparation, sample handling, sample storage and analysis associated with this voyage has been described previously (Latour et al. 2021). Briefly, all sample processing was performed inside an ISO Class 5 containerized laboratory onboard the ship. Samples for dissolved trace metal concentrations were filtered through a 0.2 µm trace-metal clean filter cartridge (AcroPak^{TM} 200, Pall). Filtered samples were then acidified using distilled (Savillex DST-1000 acid purification system) hydrochloric acid to a final pH of 1.8 and stored at room temperature until analysis. Dissolved trace metal concentrations in each sample were analysed after preconcentration and matrix removal using an automated offline seaFAST system (SC-4 DX seaFAST S2 / pico, ESI, USA) following Wuttig et al. (2019). Trace metal concentrations were determined using a Thermo Fisher ELEMENT 2 Sector Field Inductively Coupled Plasma Mass Spectrometry (SF-ICP-MS) (Central Science Laboratory, University of Tasmania). Medium spectral resolution mode was selected for the analysis of Mn and Ti. However, we expect the recovery to be lower for Ti (70-80%; Wuttig et al. 2019). Rhodium (Rh) was added as an internal standard during seaFAST processing.

The 4L discrete total particulate trace metal samples were filtered directly onboard using a custom-made filtration apparatus. Briefly, seawater was filtered through paired 25 mm acid-cleaned 0.8 µm SUPOR® (PES) filters with an effective size cut-off of 0.4 µm (Bishop et al. 2012) matching the ISPs. The filters were then digested using a mixture of strong acids (hydrochloric, nitric and hydrofluoric acid) following Bowie et al. (2010). Filters from the ISPs were subjected to a weak chemical leach, designed to extract labile trace metals from the refractory material (Berger et al. 2008). A total digestion was used to quantify the remaining refractory fraction, using the same strong acids mentioned above. Dried and resuspended digest solutions were then quantified for trace metal concentrations using SF-ICP-MS in a 10% nitric acid matrix, with indium (In) as an internal standard. Medium spectral resolution mode was selected for the analysis of pMn and particulate phosphorus (pP). Additional details about this method are described in van der Merwe et al. (2019) and Latour et al. (2021).

2.3 Hydrology

On the shelf, temperature and salinity were used to calculate neutral density and potential density, and all four parameters were used to identify different water masses (Orsi and Wiederwohl 2009; Silvano et al. 2017). Water masses of stations located over or north of the shelf break were characterised using neutral density and salinity (Pardo et al. 2017 and references therein). Both water mass characterisations can be found in Table S1. Two fronts were identified: the South Antarctic Circumpolar Front (SACCF), by the southernmost extension of oxygen minimum (Pardo et al. 2017); and the Antarctic Slope Front (ASF), as the northernmost extension of cold shelf waters (potential temperature < -1.6°C) (Rintoul 1998; Figure S1).

As part of the discussion, we calculated the proportion of Antarctic Bottom Water (AABW) and Lower Circumpolar Deep Water (LCDW) for samples within ‘bottom waters’. As these two

water masses mix along a straight line in the temperature-salinity diagram (see Figure 2 below), proportions were calculated using potential temperatures in the following equation:

$$\text{Proportion of LCDW} = \frac{\theta x - \theta AABW}{\theta x - \theta LCDW + (\theta x - \theta AABW)} \quad \text{(Equation 1)}$$

Where θ_x is the potential temperature of the depth point of interest and $\theta_{AABW}/\theta_{LCDW}$ the potential temperature endmembers of the two mixing water masses.

3. Results and Discussion

3.1 Hydrology

The potential temperature – salinity relationship reveals four water masses (Figure 2). Antarctic Surface Water (AASW), formed through warming of the surface layer during the austral summer was observed in shallow waters. Winter Water (WW), which is a cold remnant of the surface mixed layer created during the previous winter season, was observed between AASW and approximately 200 m (Silvano et al. 2017). Below the WW, Circumpolar Deep Water (CDW) occupies most of the water column below 200 m depth. The CDW is made up of two water masses with distinct water properties and origins: LCDW coincides with a deep salinity maximum and has its origins in the North Atlantic, while Upper CDW coincides with an oxygen minimum that reflects a long transit through the deep Indian and Pacific Oceans (Lynn and Reid 1968). CDW penetrates onto the shelf in some locations, where it is known as modified CDW (mCDW) because its properties are modified by mixing as it moves from the open ocean to the shelf (Orsi and Wiederwohl 2009). Finally, close to the seafloor, AABW was identified.

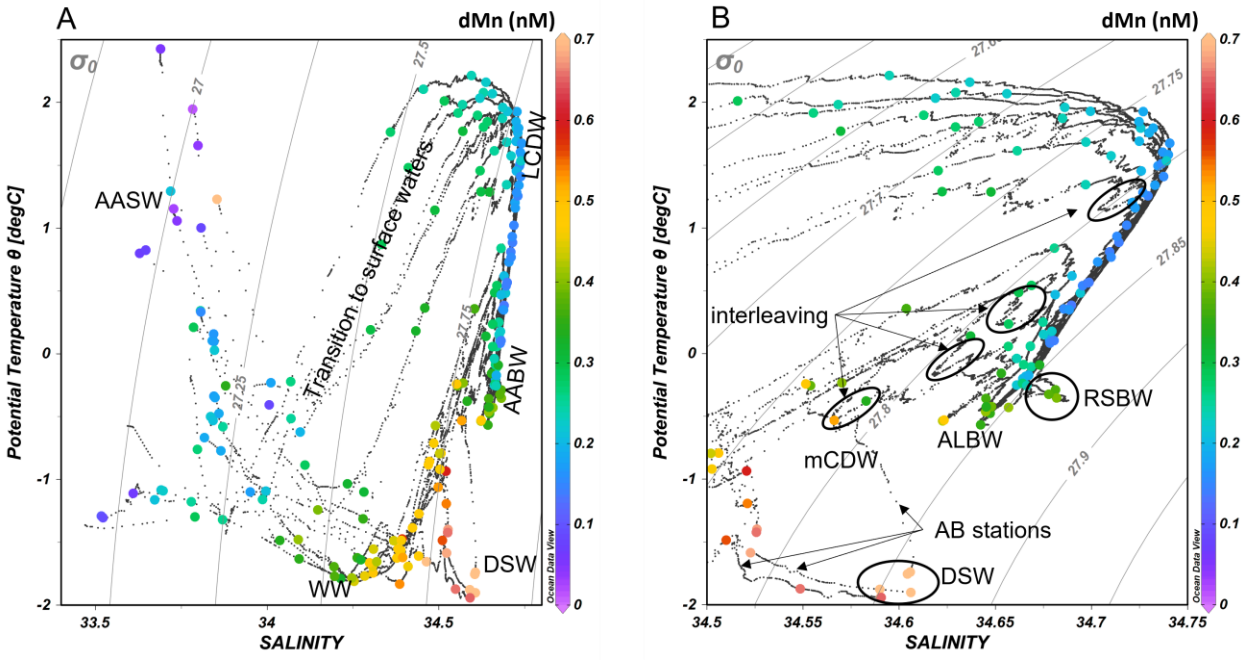

Figure 2: Potential temperature-salinity plot for a) the full dataset and b) the same dataset focusing on bottom waters, with salinities ranging from 34.5 to 34.75. Overlaid coloured dots represent dissolved Mn (dMn) concentrations. Water masses: AASW, Antarctic Surface Water; WW, Winter Water; LCDW, Lower Circumpolar Deep Water; DSW/AABW for Dense Shelf Water/Antarctic Bottom Water; mCDW, modified Circumpolar Deep Water; ALBW, Adélie Land Bottom Waters and RSBW, Ross Sea Bottom Waters.

AABW forms when Dense Shelf Water (DSW) - a cold and salty water mass formed on the continental shelf by cooling and brine rejection in winter - is exported from the shelf and mixes with CDW as it sinks to the seafloor (Gordon and Tchernia 1972). Two varieties of AABW were sampled on the voyage: relatively salty Ross Sea Bottom Water (RSBW) flowing west across 150, and a mixture of RSBW and fresher Adélie Land Bottom Water (ALBW) observed at 140 and 132 (Rintoul, 1998) (Figure 2B). The DSW that supplies ALBW is formed in the Mertz Polynya near 144°E on the Adélie Land coast. DSW with relatively high salinity (S > 34.5) was observed in some areas on the shelf near the Mertz Polynya. However, heavy sea ice prevented access to the Adélie Depression (between 142.5°E and 145°E), where the DSW contributing to ALBW formation is found (Rintoul 1998). Therefore, we cannot describe the initial (endmember) conditions of the DSW that supplies ALBW. Interleaving observed in Figure 2B indicates mixing between relatively cold, fresh and oxygen-rich waters from the Antarctic continental shelf and slope with relatively warm, salty and oxygen-poor waters offshore.

The SACCF (Orsi et al.1995) and ASF (Whitworth et al. 1985) crossed transects 132, 140 and 150. The latitude of the fronts and their separation varied between transects with the two fronts separated by a minimum of 39 km along 150 and by a maximum of 103 km along 140 (Figure 1). Southern Ocean fronts, including the SACCF and ASF, often coincide with strong lateral gradients in physical and biogeochemical properties (Orsi et al., 1995) and therefore we anticipate that their presence may influence the distribution of Mn in this region. In particular, the ASF coincides with a jump between cold, fresh waters typical of the Antarctic continental shelf/slope, and warmer, saltier offshore waters. Potential density anomalies showed that the 140 section was characterised by a strong density gradient near the ASF, highlighted by the depression in the isopycnals (Figure S1). Strong mixing is expected at the base of this feature (Jacobs 1991), and may influence water movement along this transect. Generally, higher velocity westward currents are expected over the slope, compared to shelf currents (Jacobs 1991).

Previous studies have examined the circulation of shelf water masses in this region. A combined modelling and in-situ study showed summer circulation to be dominated by a shelf wide northwestward coastal current, composed of AASW and mCDW, with limited evidence of DSW (Snow et al. 2016). A weak southeastward flow of mCDW and AASW was found to reach the shelf, east of the Adélie sill (Snow et al. 2016). This on-shelf flow of mCDW was observed at our western shelf sites, with station 39 (located at 143.64°E) composed of warmer waters at intermediate depths (Figure 2B). A slight signal of mCDW was observed at station 37. However, no such signal was observed at station 38, highlighting the spatial variability of mCDW in this region. These oceanographic differences between transects described above, namely front locations and spatial variability of water masses, may influence the distribution of Mn and other trace metals.

3.2 Manganese cycle of the Adélie and George V Lands

Dissolved Mn concentrations followed a common shape which agrees well with previous observations made in the Atlantic and Australian sectors of the Southern Ocean (further north) and in the Weddell Sea (Middag et al. 2011; Middag et al. 2013; Latour et al. 2021) (Figure 3).

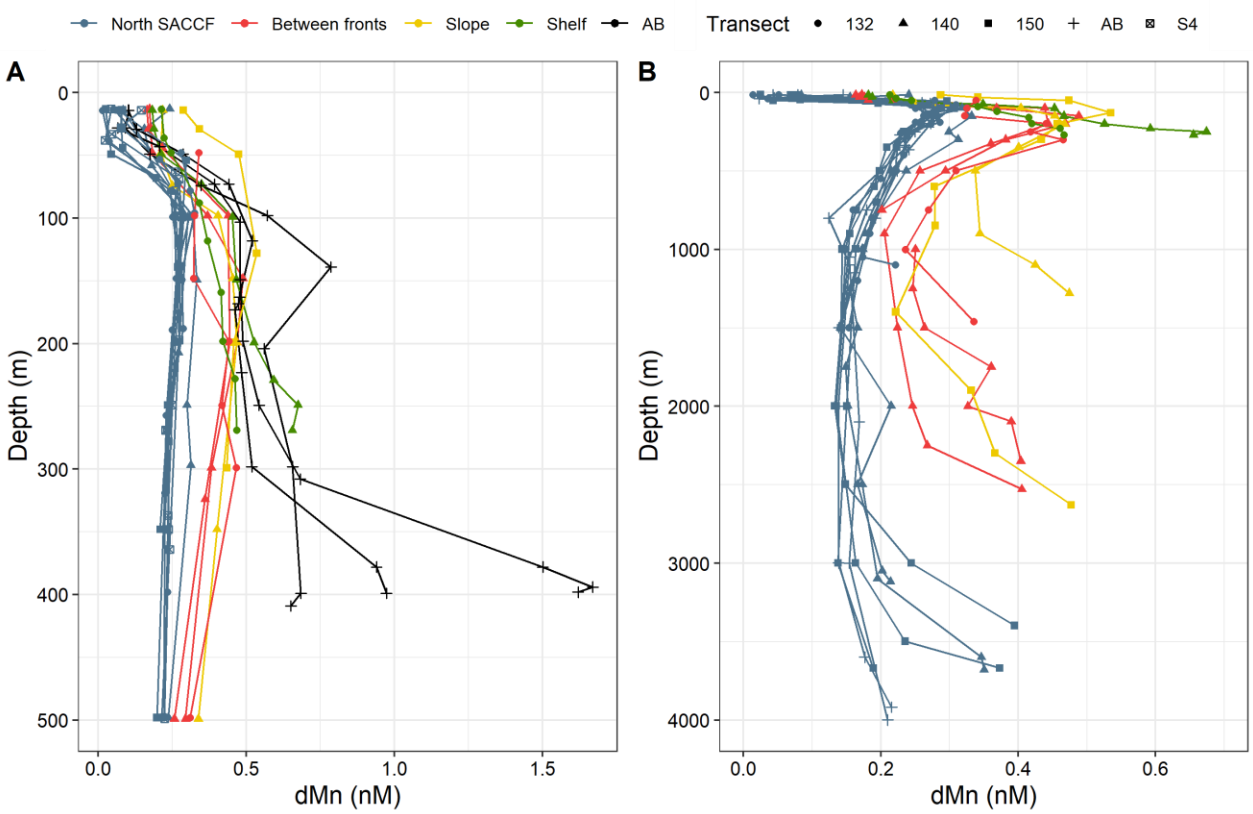

Figure 3: Depth profiles of dissolved Mn (dMn) along each transect for the first 500 m (A) and for the full depth (B). The x-axis scale of panel B was collapsed to allow the features of the depth profiles to be seen in more details. The colours represent the position of each station relative to both fronts, the slope and the shelf. The three stations near the Adélie Bank have been identified as 'AB'. These stations are not included in panel B due to their high concentrations (>0.7 nM). The symbols represent the four transects: 132, 140 and 150 (three main transects) and S4 which zonally joins all the transects.

Surface dMn concentrations were generally low, ranging on average from 0.15 nM north of the SACCF to 0.30-0.33 nM over the shelf and the slope. Along all sections, lower dMn concentrations were observed north of the SACCF with the lowest value recorded being 0.014 nM at station 47 at 14 m. To the best of our knowledge, the previous lowest open ocean dMn value recorded was 0.034 nM measured in the Drake Passage (Browning et al. 2014). Below the low surface dMn concentrations of open waters, most stations were characterized by subsurface maxima around 200 m, with peak concentrations ranging on average from 0.30 nM north of the SACCF to 0.61 nM over the shelf. These high subsurface maxima have previously been attributed to particle remineralization (Middag et al. 2011). However, little is known about these features. Below the dMn peak, decreasing concentrations were observed with depth, especially north of the SACCF (< 0.2 nM, Figure 3). Uniform low dMn distribution below subsurface maxima is commonly attributed to scavenging processes which lead to a short residence time of dMn in the deep ocean (Bruland and Lohan 2003). Near the seafloor, elevated dMn concentrations were observed at all stations (Figure 3) and may be related to either external sources or high initial Mn content in AABW (see discussion below).

Overall, increasing dMn concentrations observed toward the shelf, up to 1.5 nM, suggest the presence of strong external sources. Sediment resuspension (Lannuzel et al. 2011; 2014; Smith et al. 2021) or melting sea ice (Grotti et al. 2005) likely increase dMn shelf concentrations. However, Lannuzel et al. (2011) observed up to an order of magnitude lower dMn and pMn concentrations within sea ice relative to Fe and suggested low inputs of dMn would occur through sea ice melting in this region. Another potential source may be the supply of highly reactive sub-glacially eroded material to the shelf (e.g., Hawking et al., 2020; Bhatia et al. 2021) from the nearby Mertz and Ninnis glaciers. High ratios of refractory particulate Mn:P observed on the shelf (Table 1) support the hypothesis of recent weathering of lithogenic Mn sources (van der Merwe et al. 2019). We hypothesize that this East Antarctic region, characterized by high on-shelf Mn concentrations, may act as a source of Mn and potentially fertilise depleted open ocean waters, as previously seen in the Drake Passage (Measures et al. 2013). To study the potential export of Mn-enriched waters from this region, we assumed that if dMn is transported within a specific water mass, it may follow a dilution mixing line. By using salinity as a conservative tracer, we looked at the evolution of dMn, salinity and the ratio between dMn and salinity with distance from the coast to verify this (Figure 4).

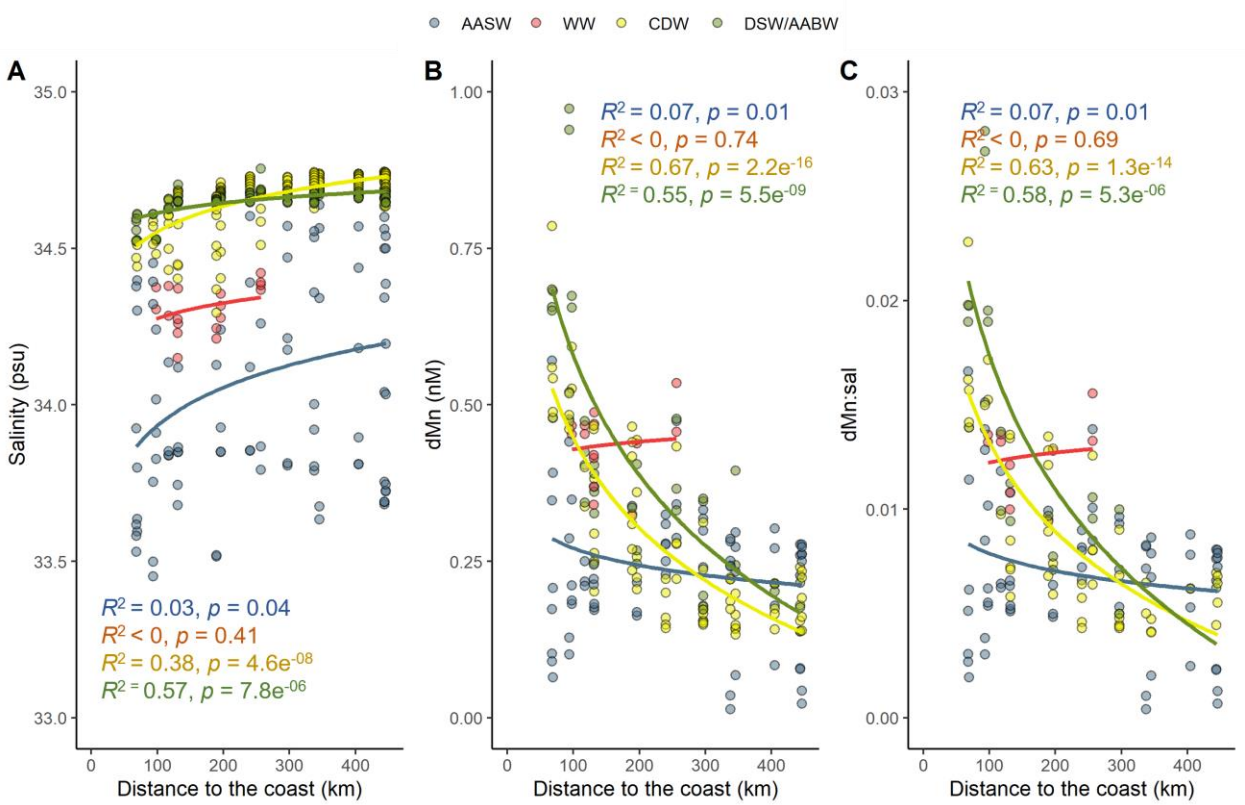

Figure 4: Scatter plot showing the evolution of salinity (A), dMn (B) and the ratio between dMn:salinity (C) with distance from the coast (in km). Logarithmic regression lines are added with the corresponding R^2 and p value. Colours represent the water masses: AASW, Antarctic Surface Water (blue); WW, Winter Water (red); CDW, Circumpolar Deep Water (yellow); and DSW/AABW for Dense Shelf Water/Antarctic Bottom Water (green).

We observed a decrease in dMn concentrations with distance from the coast for all water masses except WW while salinity remained relatively constant in comparison (Figure 4A, B). The largest variations in salinity were observed in AASW and may be related to sea ice melting

(Duprat et al. 2020). The ratio of dMn per unit of salinity followed the trend of dMn (Figure 4C), indicating that processes other than dilution specifically impact dMn distribution by decreasing its concentration with distance from the coast. This may include biological uptake as well as scavenging (see discussion below). Considering our aim to study the export of dMn from this East Antarctic region, we focused our investigation on water masses subjected to northward travel; the AASW and DSW/AABW (Snow et al. 2016; Foppert et al. 2021; see section 3.1). Accordingly, subsequent discussion is divided into two sections focusing on processes limiting Mn export ('Biological uptake in surface waters' and 'Removal of dMn in bottom waters') before attempting to quantify Mn lateral export ('Export of Mn-enriched waters').

Biological uptake in surface waters

Southern Ocean dMn distribution is commonly characterized by low surface concentrations attributed to biological uptake and few external sources (Klinkhammer and Bender 1980; Middag et al. 2011). In this study, we observed low surface dMn concentrations at all stations but the lowest values (< 0.1 nM) were recorded north of the SACCF (Figure 3A). By combining chlorophyll fluorescence (F_o), PAR and transmittance; NPQ can be identified in surface waters on days of high light intensity (stations 44, 46 and 47) yet transmittance highlights a well-mixed layer down to 40 m (Figure 5). Therefore, F_o and transmittance at 40 m (below the depth where NPQ reduces F_o) can be used as proxies for phytoplankton biomass. While F_o was inversely correlated with dMn north of the SACCF (R^2 = 0.20; p = 0.15), transmittance versus dMn reveals a significant positive correlation (R^2 = 0.49; p = 0.03), most likely caused by biological uptake of dMn.

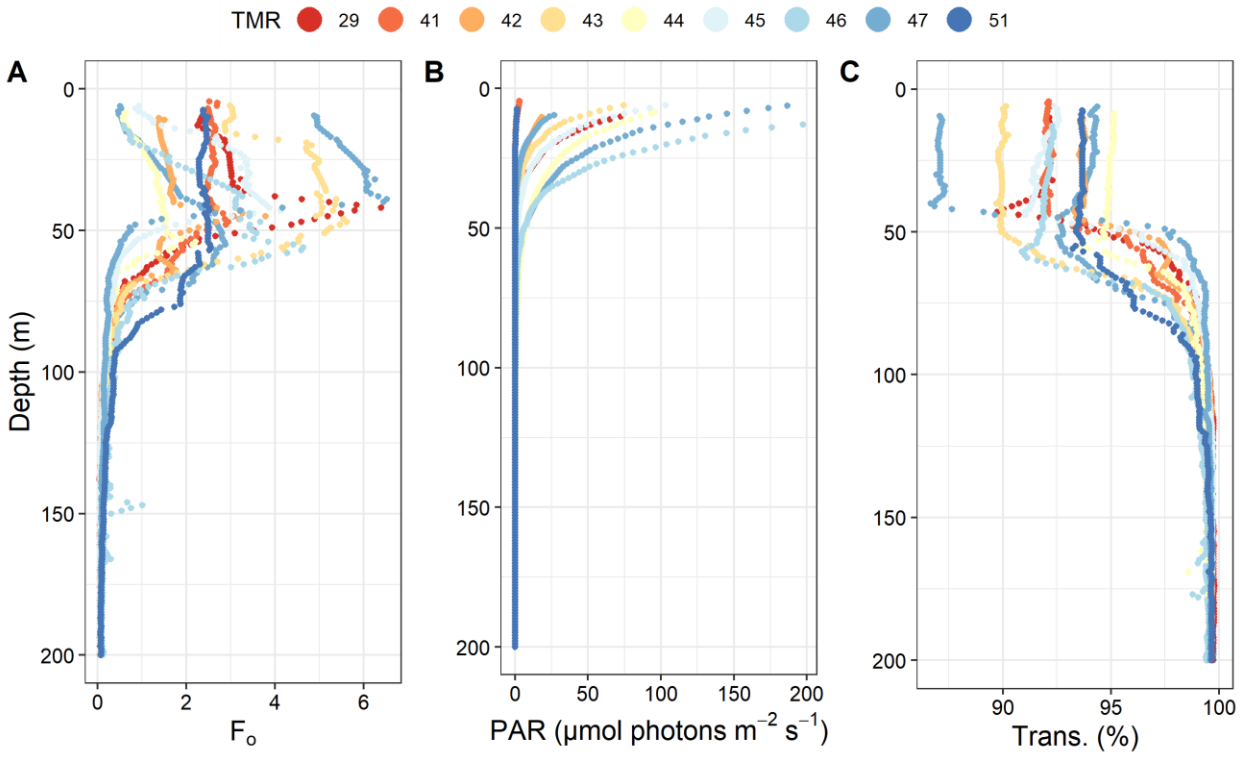

Figure 5: Depth profiles of fluorescence (F_o) (a), Photosynthetic Active Radiation (PAR in µmol photons m^{-2} sec^{-1}) (b) and transmittance (%) (c) between 0-200 m, north of the SACCF where the lower surface dMn concentrations were observed.

In addition, ratios between Mn, PO_4^{3-}/P and Ti supported the hypothesis of increasing biological uptake with distance from the coast (Table 1). Lower dissolved Mn:PO_4^{3-} and Mn:Ti ratios were observed in the northern region of the study while conversely, increasing total particulate Mn:Ti ratios were observed with distance from the coast. This particulate Mn enrichment relative to Ti combined with the decrease in dMn ratios suggests a transfer of Mn from the dissolved toward the particulate fraction, which may indicate: i) biological uptake; ii) formation of Mn oxides; iii) scavenging of dMn onto particles; or iv) a combination of these. In addition, the decrease in total particulate Mn:P ratio with distance from the coast combined with the increase in labile pMn (Table 1) supported the hypothesis of increasing biological influence over the Mn cycle with distance from the coast. Diatoms and Phaeocystis sp. have been observed to increase their Mn requirement under Fe stress (Peers and Price 2004) or to accumulate Mn in their mucilage in the case of Phaeocystis (Davidson and Marchant, 1987). Therefore, surface dMn may have been depleted and transferred into the particulate phase after a bloom of such species. Profiles of silicic acid concentrations with depth showed depleted surface levels at stations 47 and 51, supporting the hypothesis of dMn drawdown resulting from diatom growth (Figure S2). Nitrate (NO_3^-) to PO_4^{3-} (NO_3^-:PO_4^{3-}) ratios, which may indicate the dominance of one phytoplankton group over the other (e.g. diatoms vs Phaeocystis), remain intermediate north of the SACCF (ranging from 15.2 to 16.4) and therefore could not be used as an additional proxy of phytoplankton community composition (Arrigo et al. 2015).

Table 1: Dissolved and particulate Mn concentrations along with various ratios in the dissolved, total and labile particulate fractions between Mn, PO_4^{3-}/P and Ti, measured in surface waters (above the dMn subsurface maxima as described in Middag et al. 2011). All ratios are presented in mol mol^{-1} except for the dMn:dPO_4^{3-} ratios which are in mmol mol^{-1}.

Fraction	Parameter	Shelf	Slope	Between fronts	North SACCF
Dissolved	dMn (nM)	0.31 ± 0.17	0.33 ± 0.11	0.29 ± 0.11	0.15 ± 0.10
	dMn:dPO_4^{3-}	0.149 ± 0.07	0.174 ± 0.04	0.14 ± 0.04	0.074 ± 0.04
	dMn:dTi	0.045 ± 0.03	0.039 ± 0.01	0.041 ± 0.02	0.022 ± 0.01
Total particulate	pMn (nM)	0.023 ± 0.01	-	0.03 ± 0.01	0.04 ± 0.02
	pMn:pP	1.91 ± 2.21	-	1.37 ± 1.5	0.47 ± 0.20
	pMn:pTi	0.177 ± 0.06	-	1.03 ± 0.99	2.85 ± 1.73
Labile:tot. particulate	LpMn:totpMn	42.7 ± 5	50.4 ± 7	42.4 ± 15	57.9 ± 10

Sea ice coverage is expected to influence the start of the bloom season. When the ice melts, increased light and nutrient availability will favour phytoplankton growth (Deppeler and Davidson 2017). Surface dMn concentrations may first increase due to sea ice melt (Lannuzel et al. 2014), but uptake by phytoplankton should then lead to decreasing dMn and other trace metal concentrations throughout the bloom season (Kanna et al. 2020). Here, sea ice had melted north of the SACCF prior to our occupation along all three longitudinal transects, as shown by the sea ice persistence (Figure 1B). These results imply phytoplankton uptake started earlier north of the SACCF along each transect and agree with the observed lower dMn concentrations (Figure 3A).

Nonetheless, sea ice movement represents a potential source of Mn and other trace metals as it may transport nutrients north of the SACCF and locally stimulate phytoplankton growth (Kanna et al. 2020). These local inputs are expected to vary seasonally with higher local enrichment/fertilization in the early season (austral spring/summer). Sea ice advection for the period of this study indicated sea ice was carried eastward by the ACC (Figure 1B). Hence, sea ice coming from the west of this region could potentially increase local trace metal concentrations.

Removal of dissolved manganese in bottom waters

The sharpest decrease in dMn with distance from the coast was observed in bottom waters (Figure 4C). This suggested one or several process(es) decrease dMn concentrations in AABW, which was surprising considering dMn concentrations are often hypothesized to increase near the seafloor due to inputs from sediment resuspension or redox mobilization (Middag et al. 2011; Cheize et al. 2019; Morton et al. 2019). Since biological uptake is unlikely at these depths, we derive two hypotheses from this observation: i) one or several process(es) remove(s) dMn in bottom waters and ii) the elevated dMn concentrations observed near the seafloor (Figure 3) originate from the shelf and are carried downstream with the flow of AABW (and not from constant sediment inputs, otherwise AABW dMn:salinity ratio would increase with distance from the coast). Considering the removal hypothesis, dMn decrease may result from two processes: 1) scavenging of dMn onto particles and/or 2) dilution of dMn-rich AABW with overlying Mn-depleted LCDW. To separate these processes, the fraction of LCDW within AABW was calculated at each location where we have dMn data. We used the temperature endmembers within the cores of AABW and LCDW (identified in Figure 2A) as inputs for the equation (Figure 6). Salinity presented the same trend but with a lesser dynamic range (data not shown here).

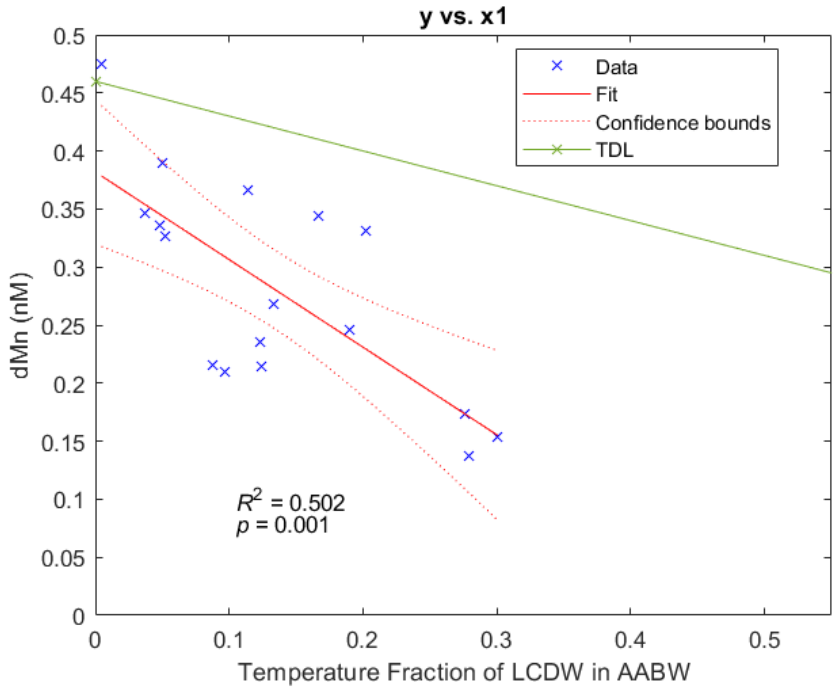

Figure 6: Dissolved manganese (dMn) concentrations measured in Antarctic Bottom Water (AABW) against the fraction of Low Circumpolar Deep Water (LCDW) in AABW. Linear regression with 95% confidence interval, R^2

and p value are displayed. The theoretical dilution line (TDL) is shown for a theoretical mixture of AABW and LCDW with dMn endmembers set as the mean of all off-shelf dMn observations within each water mass. The TDL assumes no losses or enrichments during mixing.

Results indicated that as the contribution of LCDW increased in AABW samples, the associated dMn concentrations decreased (Figure 6). This result suggests that dilution of AABW with the overlying LCDW partly controls the concentrations of dMn in our observations. However, almost all measurements of dMn concentrations in AABW are lower than the theoretical dilution line (TDL; Figure 6). This suggests that final dMn concentrations are lower than expected strictly from the mixing of these water masses (0.30 – 0.45 nM), and indicate an additional removal process occurs. We hypothesize this additional loss of dMn results from scavenging processes.

Scavenging implies an adsorption of dMn onto particles, transferring Mn from the dissolved into the particulate phase (Bruland and Lohan 2003). With distance from the coast, pMn concentrations within DSW/AABW remained relatively stable with local higher concentrations on the shelf (Figure S3). This is in agreement with high particle content near the Antarctic shelf, where sources of Mn are abundant (Sherrell et al. 2018; Smith et al. 2021). The high fraction of refractory pMn observed on the shelf and gradual reduction in the proportion of refractory material with distance from the coast (Figure 7) suggest that higher density particles settle out to sediments preferentially, whereas lower density, labile (often biogenic/detritus) particles remain suspended in AABW (van der Merwe et al. 2019).

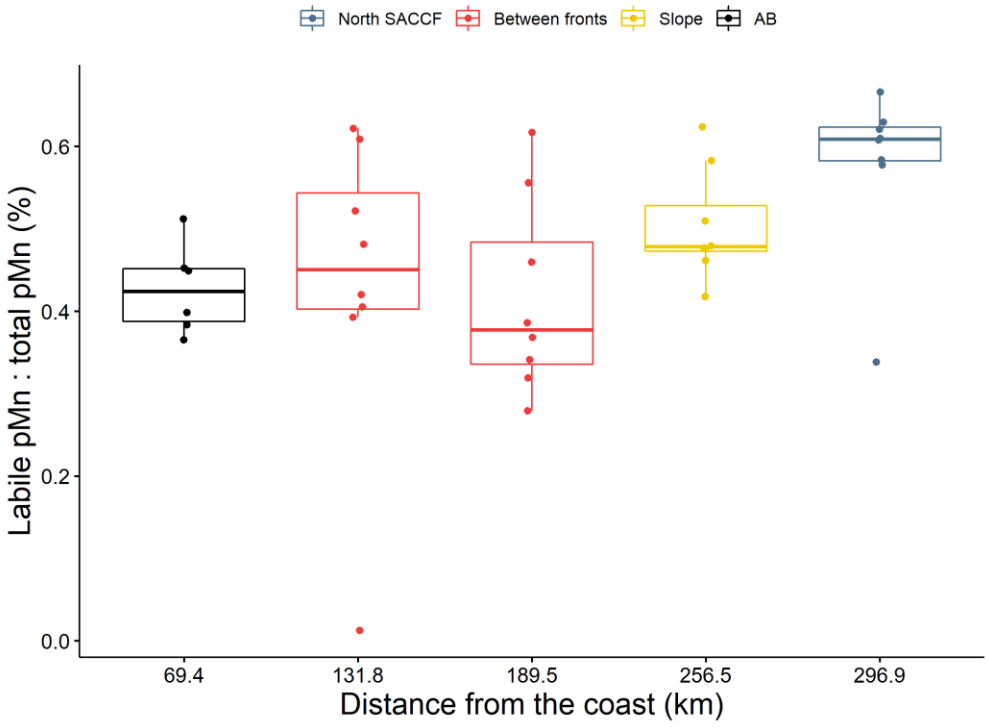

Figure 7: Ratio between labile particulate manganese to total particulate manganese in % with distance from the coast (in km). The colours represent the stations position relative to both fronts, the slope and the shelf.

When not associated with refractory material, pMn is often primarily composed of Mn oxides, which are known as strong scavengers, able to decrease surrounding dMn and other trace metal concentrations (Goldberg 1954; Tonkin et al. 2004). Near the seafloor, it was previously

demonstrated that Mn oxides precipitate within sediment under high oxygen concentrations, leading to decreasing dMn concentrations in the overlaying water (Sundby et al. 1986). This is likely occurring in this region as AABW is characterized by high oxygen content (>230 µM) (Rintoul 1998). Formation of Mn oxides can occur under both biotic or abiotic influence (Sunda and Huntsman 1988). However, abiotic Mn(II) oxidation is known to be much slower compared to the microbially-mediated Mn(II) oxidation. Consequently, most Mn oxides are usually considered biogenic (Sunda and Huntsman 1988; Morgan 2005). Rates of Mn(II) oxidation have not yet been determined in this region, although a recent study observed a lack of Mn oxides in the Ross Sea, attributed to a unique Mn redox cycle and persistence of Mn(III) ligands complexes (Oldham et al. 2021). In the present study, conservative or increasing dMn depth-profiles were also observed over the shelf (Figure 3A), suggesting either that i) dMn sources and inputs compensate for dMn loss by scavenging or that ii) this East Antarctic region may also be characterized by low scavenging rates on the shelf, associated with low abundance of Mn oxides (Oldham et al. 2021). In the deep ocean, microbially-mediated Mn(II) oxidation rates have been observed to vary, especially within hydrothermal plumes with faster reactions compared to surrounding background waters, resulting from different bacterial communities (Dick et al. 2009). Hence, biotic scavenging rates may vary widely between coastal and offshore regions and also depend on the composition of microbial communities. Estimating Mn(II) oxidation rates remains necessary to quantify scavenging processes and evaluate the potential export of dMn within AABW in this region.

Lateral export of Mn-enriched waters

The primary aim of this study was to identify if this East Antarctic region may act as a source of dMn for depleted Southern Ocean waters further north. Despite high dMn concentrations observed over the shelf, our results suggest dMn export from this region is limited, particularly in surface waters. We suggest biological uptake reduces surface dMn concentrations, while mixing with overlying depleted-waters and scavenging limit export of dMn within bottom waters. Overall, we observed that waters transported north of the SACCF were low in dMn (0.1 nM in AASW, 0.2 nM in AABW; Figure 3). These values are in agreement with the study from Middag et al. (2011), which measured similar surface concentrations in the Weddell Gyre. This suggests limited export of dMn may occur around Antarctic regions. However, we suggest the horizontal advection of subsurface Mn-enriched waters (150 - 300 m) may constitute the major source of dMn for surface waters following strong wind-mixing and/or upwelling induced by eddies (Patel et al. 2020).

Subsurface dMn maxima are common features of the Southern Ocean (Middag et al. 2011). At all stations, we observed subsurface dMn maxima located between 73 to 300 m with higher values recorded near the shelf (Figure S4). This East Antarctic region is characterized by a shelf depth varying between 200 and 400 m (Beaman et al. 2011) which suggests that processes on the shelf provide a source of dMn at intermediate depth and could partly explain the presence of subsurface dMn maxima in Southern Ocean waters (Smith et al. 2021). The identification of these features further north indicate this Mn-enriched plume may travel great distance at intermediate depths (Middag et al. 2011; Latour et al. 2021). Similar subsurface features were observed in the Western Antarctic Peninsula and attributed to sediment inputs (Sherrell et al. 2018). However, previous studies associated these dMn subsurface maxima with remineralization of particulate organic matter (Middag et al. 2011). It is likely that both processes - lateral advection of Mn-enriched waters and particle remineralization - help maintain

these subsurface features at intermediate depths, with the contribution from each source varying depending on proximity to shelf regions. In the present study, lower oxygen concentrations measured near these subsurface maxima support the hypothesis that particles are remineralized at those depths (Figure 8). Concurrent increase of dMn concentrations with decreasing oxygen levels are well documented, especially in oxygen minimum zones where the reductive dissolution of Mn oxides lead to the accumulation of Mn(II) (Lewis and Luther 2000).

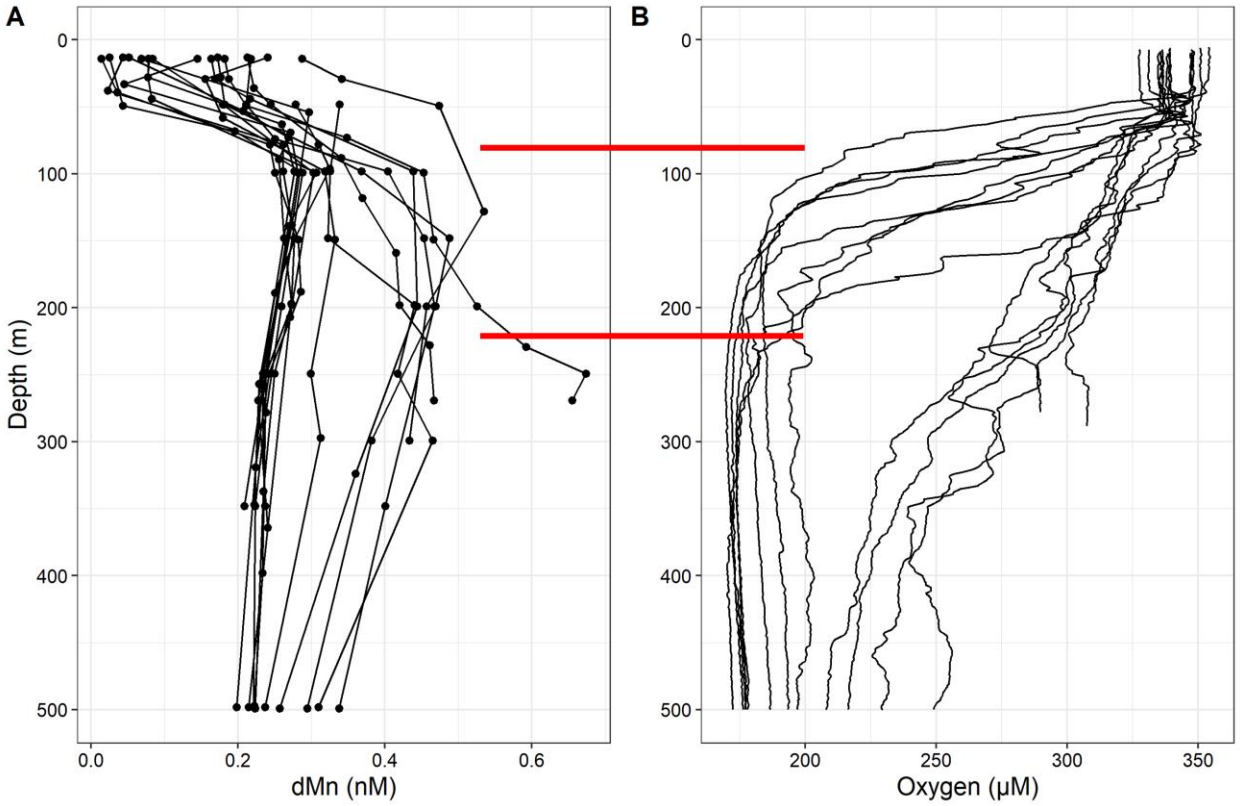

Figure 8: Depth profiles of dissolved Mn (dMn in nM, A) and oxygen concentrations (in µM, B) between 0-500 m for all TMR stations, except the three Adélie Bank stations. The two red lines indicate coincident low oxygen concentrations with relatively high dMn concentrations.

Estimating a precise budget and flux of dMn from this region remains complex. Overall, our data suggest dMn export is limited in both surface and bottom waters. However, the advection of high dMn concentrations (double the amount of surface waters) via subsurface maxima constitute a potential important source for surface waters following strong-wind-mixing and/or upwelling (Figure 9). Considering bottom water transport, the main limitation of this study resides in the fact that we did not follow the path of a specific AABW plume pathway. Instead, the three latitudinal transects we sampled cut across several AABW plumes (Figure 1A; Foppert et al. 2021). To further confirm the hypothesis of dMn loss within bottom waters, it remains essential to follow a specific plume, while characterizing particle composition and Mn(II) oxidation rates.

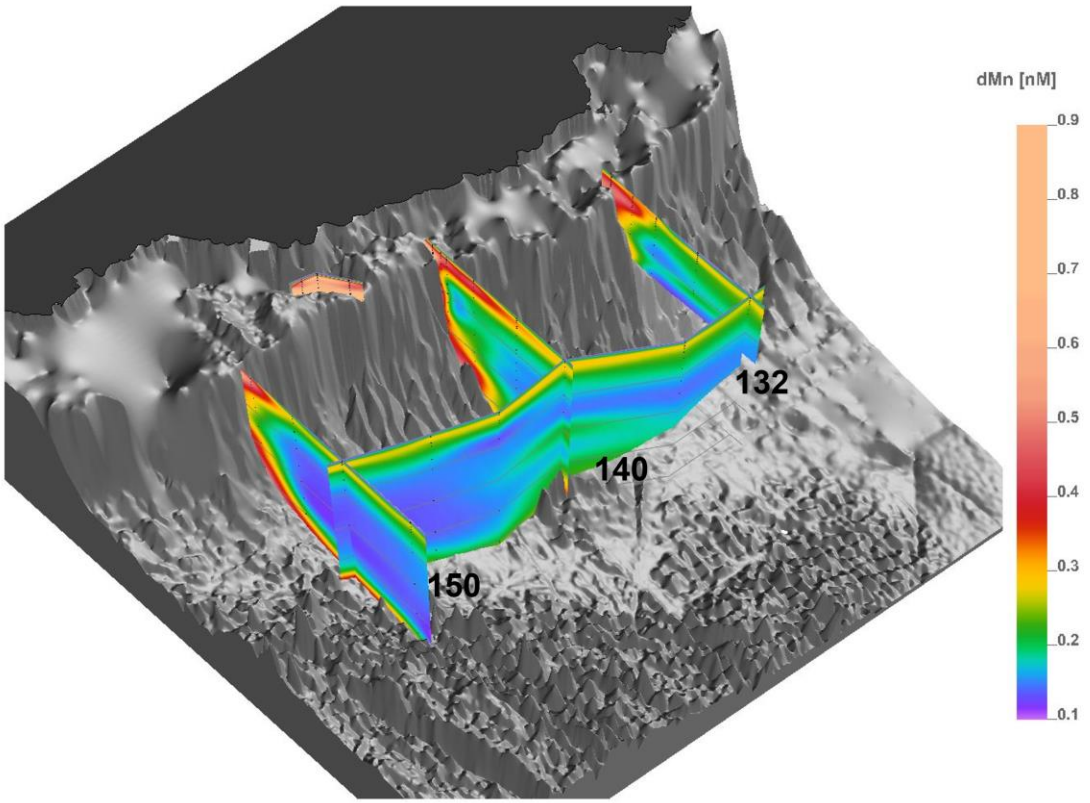

Figure 9: 3D plot showing dissolved Mn (dMn) concentrations (in nM) along the three perpendicular sections measured (132, 140 and 150). While dMn was elevated in bottom waters, we observed a decrease of dMn with distance from the coast. We suggest subsurface dMn maxima may be an important source of dMn for surface waters.

4. Conclusions

We investigated the potential northward export of Mn-enriched Antarctic shelf waters. High Mn concentrations were found on the shelf and were likely attributed to sediment and glacial discharge sources. We found that dMn export in surface waters was limited due to biological uptake and dMn concentrations strongly decreased north of the SACCF. This sharp decrease in Mn was linked to the timing of sea ice melting, which occurs earlier in spring north of the SACCF and stimulates phytoplankton growth and uptake of bioessential trace metals. We observed a subsurface dMn maximum at all stations north of the shelf break and suggest it may be linked to the combination of particle remineralization and advection of Mn-enriched Antarctic shelf waters at those depths. After factoring in dilution of AABW with overlying LCDW, export of dMn via bottom water formation and advection off the shelf is hypothesized to be limited by both Mn(II) oxidation and scavenging associated with Mn oxides. This result was surprising due to the expectation that input from sediments would enrich AABW dMn concentrations as it travels away from the shelf. Overall, export of Mn-enriched waters toward Southern Ocean open waters is limited in this region, an observation that is likely to also be the case for other areas around the Antarctic continent. These results improve our understanding of the Southern Ocean's status as an HNLC region and relate to previous studies which measured very low Mn concentrations in open waters of this region. This lack of Mn export may have implications regarding phytoplankton growth (co-)limitation by Mn throughout the broader Southern Ocean,

but also by other important biologically essential trace metals previously expected to be exported northward alongside Mn, such as Fe.

Acknowledgments

We would like to acknowledge the officers and crew of the RV Investigator (Australian Marine National Facility) for the deployment of all the instruments during the GEOTRACES GS01 voyage (IN2018-V01), and the hydrochemistry team who performed the macronutrients and oxygen analyses onboard. We thank Morgane Perron for her help during the trace metal sampling processing along the voyage. This work was funded through receipt of Australian Research Council grants FT130100037 (to ARB), LE0989539 (to ATT and ARB for analysis), by the Antarctic Climate & Ecosystems Cooperative Research Centre (ACE CRC) and by the Australian Marine National Facility. This work was also partly supported by the Antarctic Science Collaboration Initiative through the Australian Antarctic Program Partnership (AAPP) and by the Centre for Southern Hemisphere Oceans Research, a partnership between CSIRO, the Qingdao National Laboratory for Marine Science and Technology, the University of Tasmania and the University of New South Wales.

Open Research

Trace metal data used for this study can be found in the GEOTRACES Intermediate Data Product (IDP2021; https://www.geotraces.org/geotraces-intermediate-data-product-2021/). Data for oceanography can be found on the Marine National Facility Marlin website (https://mnf.csiro.au/en/MNF-Data).

References

Aguilar-Islas, A. M., and Bruland K. W. 2006. "Dissolved Manganese and Silicic Acid in the Columbia River Plume: A Major Source to the California Current and Coastal Waters off Washington and Oregon." Marine Chemistry 101 (3–4): 233–47. https://doi.org/10.1016/j.marchem.2006.03.005.

Angino, E. 1966. "Geochemistry of Antarctic Pelagic Sediments," Geochimica et Cosmochimica Acta, 1966, vol. 30, no 9, p. 939-961.

Armstrong, F. A. 2008. "Why Did Nature Choose Manganese to Make Oxygen?" Philosophical Transactions of the Royal Society B: Biological Sciences 363 (1494): 1263–70. https://doi.org/10.1098/rstb.2007.2223.

Arrigo, K. R., van Dijken, G. L., and Strong A. L. 2015. "Environmental Controls of Marine Productivity Hot Spots around Antarctica." Journal of Geophysical Research: Oceans 120 (8): 5545–65. https://doi.org/10.1002/2015JC010888.

Beaman, R. J., E. O'Brien, P., Post, A. L., and De Santis, L. 2011. "A New High-Resolution Bathymetry Model for the Terre Adélie and George V Continental Margin, East Antarctica." Antarctic Science 23 (1): 95–103. https://doi.org/10.1017/S095410201000074X.

Berger, C. J. M., Lippiatt, S. M., Lawrence, M. G., and Bruland, K. W. 2008. "Application of a Chemical Leach Technique for Estimating Labile Particulate Aluminum, Iron, and Manganese in the Columbia River Plume and Coastal Waters off Oregon and Washington." Journal of Geophysical Research 113 (August): C00B01. https://doi.org/10.1029/2007JC004703.

549 Bhatia, M. P., Waterman, S., Burgess, D. O., Williams, P. L., Bundy, R. M., Mellett, T., Roberts,
550 M. and E. R. Bertrand. 2021. Glaciers and nutrients in the Canadian Arctic Archipelago
551 marine system. Global Biogeochemical Cycles, 2021, vol. 35, no 8, p. e2021GB006976.
552
553 Bishop, J. K.B., Lam Phoebe J., and Todd J. Wood. 2012. "Getting Good Particles: Accurate
554 Sampling of Particles by Large Volume in-Situ Filtration: Getting Good Particles."
555 Limnology and Oceanography: Methods 10 (9): 681–710.
556 https://doi.org/10.4319/lom.2012.10.681.
557 Bowie, A. R., Lannuzel, D., Remenyi, T. A., Wagener, T., Lam, P. J., Boyd, P. W., Guieu, C.,
558 Townsend, A. T., and Trull, T. W. 2009. "Biogeochemical Iron Budgets of the Southern
559 Ocean South of Australia: Decoupling of Iron and Nutrient Cycles in the Subantarctic
560 Zone by the Summertime Supply." Global Biogeochemical Cycles 23 (4): n/a-n/a.
561 https://doi.org/10.1029/2009GB003500.
562 Bowie, A. R., Townsend, A. T., Lannuzel, D., Remenyi, T. A., and van der Merwe, P. 2010.
563 "Modern Sampling and Analytical Methods for the Determination of Trace Elements in
564 Marine Particulate Material Using Magnetic Sector Inductively Coupled Plasma–Mass
565 Spectrometry." Analytica Chimica Acta 676 (1–2): 15–27.
566 https://doi.org/10.1016/j.aca.2010.07.037.
567 Boyd, P. W., Watson, A. J., Law, C. S., Abraham, E. R., Trull, T. W., Murdoch, R., Bakker, D.
568 C. E., et al. 2000. "A Mesoscale Phytoplankton Bloom in the Polar Southern Ocean
569 Stimulated by Iron Fertilization." Nature 407 (6805): 695–702.
570 https://doi.org/10.1038/35037500.
571 Browning, T. J., Bouman, H. A., Henderson, G. M., Mather, T. A., Pyle, D. M., Schlosser, C.,
572 Woodward, E. M. S., and Moore, C. M. 2014. "Strong Responses of Southern Ocean
573 Phytoplankton Communities to Volcanic Ash." Geophysical Research Letters 41 (8):
574 2851–57. https://doi.org/10.1002/2014GL059364.
575 Browning, T. J., Achterberg, E. P., Engel, A., and Mawji, E. 2021. "Manganese Co-Limitation of
576 Phytoplankton Growth and Major Nutrient Drawdown in the Southern Ocean." Nature
577 Communications 12 (1): 884. https://doi.org/10.1038/s41467-021-21122-6.
578 Bruland, K W, and M C Lohan. 2003. "6.02 Controls of trace metals in seawater," Treatise on
579 geochemistry, vol. 6, p.625.
580 Cheize, M., Planquette, H.F., Fitzsimmons, J.N., Pelleter, E., Sherrell, R.M., Lambert, C.,
581 Bucciarelli, E., Sarthou, G., Le Goff, M., Liorzou, C., Chéron, S., Viollier, R. and Gayet,
582 N. 2019. "Contribution of Resuspended Sedimentary Particles to Dissolved Iron and
583 Manganese in the Ocean: An Experimental Study." Chemical Geology 511 (April): 389–
584 415. https://doi.org/10.1016/j.chemgeo.2018.10.003.
585 Corami, F., Capodaglio, G., Turetta, C., Soggia, F., Magi, E., and Grotti, M. 2005. "Summer
586 Distribution of Trace Metals in the Western Sector of the Ross Sea, Antarctica." Journal
587 of Environmental Monitoring 7 (12): 1256. https://doi.org/10.1039/b507323p.
588 Cutter, G., Casciotti, K., Croot, P., Geibert, W., Heimbürger, L-E., Lohan, M., Planquette, H. and
589 van de Flierdt, T. 2017. "Sampling and Sample-Handling Protocols for GEOTRACES
590 Cruises."

591 Davidson, A. T., and Marchant, H. J. 1987. “Binding of manganese by Antarctic Phaeocystis
592 pouchetii and the role of bacteria in its release". Marine biology, vol. 95, no 3, p. 481-
593 487.

594 Deppeler, S. L., and Davidson, A. T. 2017. “Southern Ocean Phytoplankton in a Changing
595 Climate.” Frontiers in Marine Science 4 (February).
596 https://doi.org/10.3389/fmars.2017.00040.

597 Dick, G. J., Clement, B. G., Webb, S. M., Fodrie, F. J., Bargar, J. R., & Tebo, B. M. (2009).
598 Enzymatic microbial Mn (II) oxidation and Mn biooxide production in the Guaymas
599 Basin deep-sea hydrothermal plume. Geochimica et Cosmochimica Acta, 73(21), 6517-
600 6530.

601 Duprat, L., Corkill, M., Genovese, C., Townsend, A. T., Moreau, S., Meiners, K. M., and
602 Lannuzel, D. 2020. “Nutrient Distribution in East Antarctic Summer Sea Ice: A Potential
603 Iron Contribution From Glacial Basal Melt.” Journal of Geophysical Research: Oceans
604 125 (12). https://doi.org/10.1029/2020JC016130.

605 Fitzwater, S.E, Johnson, K. S., Gordon, R.M., Coale, K.H., and Smith, W.O. 2000. “Trace Metal
606 Concentrations in the Ross Sea and Their Relationship with Nutrients and Phytoplankton
607 Growth.” Deep Sea Research Part II: Topical Studies in Oceanography 47 (15–16):
608 3159–79. https://doi.org/10.1016/S0967-0645(00)00063-1.

609 Foppert, A., Rintoul, S. R., Purkey, S. G., Zilberman, N., Kobayashi, T., Sallèe, J-B., E. Wijk,
610 M., and Wallace, L. O. 2021. “Deep Argo Reveals Bottom Water Properties and
611 Pathways in the Australian-Antarctic Basin.” Journal of Geophysical Research: Oceans
612 126 (12). https://doi.org/10.1029/2021JC017935.

613 Goldberg, E. D. 1954. “Marine Geochemistry 1. Chemical Scavengers of the Sea.” The Journal
614 of Geology 62 (3): 249–65. https://doi.org/10.1086/626161.

615 Gordon, A. L., and P. Tchernia. 1972. Waters of the continental margin off Adélie coast,
616 Antarctica, in Antarctic Oceanology II: The Australian-New Zealand Sector, Antarct.
617 Res. Ser., vol. 19, edited by D. E. Hayes, pp. 59–69, AGU, Washington, D. C.

618 Grotti, M., Soggia, F., Ianni, C., and Frache, R. 2005. “Trace Metals Distributions in Coastal Sea
619 Ice of Terra Nova Bay, Ross Sea, Antarctica,” Antarctic Science, 2005, vol. 17, no 2, p.
620 289-300.12.

621 Hawkings, J. R., Skidmore, M. L., Wadham, J. L. et al. 2020. “Enhanced trace element
622 mobilization by Earth's ice sheets." Proceedings of the National Academy of Sciences.
623 vol. 117, no 50, p. 31648-31659.

624 Holmes, T. M., Chase, Z., Townsend, A. T., and Bowie A. R. 2017. “Detection, Dispersal and
625 Biogeochemical Contribution of Hydrothermal Iron in the Ocean,” Marine and
626 Freshwater Research, 2017, vol. 68, no 12, p. 2184-2204.

627 Horton, P., Ruban, A. V., and Walters R. G.. 1996. “Regulation of light harvesting in green
628 plants.” Annual Review of Plant Physiology and Plant Molecular Biology 47 (1): 655–84.
629 https://doi.org/10.1146/annurev.arplant.47.1.655.

630 Jacobs, S. S. 1991. “On the Nature and Significance of the Antarctic Slope Front.” Marine
631 Chemistry 35 (1–4): 9–24. https://doi.org/10.1016/S0304-4203(09)90005-6.

Kanna, N., Lannuzel, D., van der Merwe, P., and Nishioka, J. 2020. "Size Fractionation and Bioavailability of Iron Released from Melting Sea Ice in a Subpolar Marginal Sea." Marine Chemistry 221 (April): 103774. https://doi.org/10.1016/j.marchem.2020.103774.

Kimura, N. 2004. Sea ice motion in response to surface wind and ocean current in the Southern Ocean. Journal of the Meteorological Society of Japan. Ser. II, 82(4), 1223-1231. doi:10.2151/jmsj.2004.1223.

Klinkhammer, G. P., and Bender, M. L. 1980. "The distribution of manganese in the Pacific Ocean". Earth and Planetary Science Letters, 1980, vol. 46, no 3, p. 361-384.

Lannuzel, D., Bowie, A. R., Remenyi, T., Lam P., Townsend, A. T., Ibisanmi, E., Butler, E., Wagener, T., and Schoemann, V. 2011. "Distributions of Dissolved and Particulate Iron in the Sub-Antarctic and Polar Frontal Southern Ocean (Australian Sector)." Deep Sea Research Part II: Topical Studies in Oceanography 58 (21–22): 2094–2112. https://doi.org/10.1016/j.dsr2.2011.05.027.

Lannuzel, D., van der Merwe, Pier C., Townsend, A. T., and Bowie, A. R. 2014. "Size Fractionation of Iron, Manganese and Aluminium in Antarctic Fast Ice Reveals a Lithogenic Origin and Low Iron Solubility." Marine Chemistry 161 (April): 47–56. https://doi.org/10.1016/j.marchem.2014.02.006.

Latour, P., Wuttig, K., van der Merwe, P., Strzepek, R. F., Gault-Ringold, M., Townsend, A. T., Holmes, T. M., Corkill, M. and Bowie, A. R. 2021. "Manganese Biogeochemistry in the Southern Ocean, from Tasmania to Antarctica," Limnology and Oceanography, 66: 2547-2562. https://doi.org/10.1002/lno.1177216.

Lewis, B. L., and Luther III, G. W. 2000. Processes controlling the distribution and cycling of manganese in the oxygen minimum zone of the Arabian Sea. Deep Sea Research Part II: Topical Studies in Oceanography, 47(7-8), 1541-1561.

Liniger, G., Strutton, P. G., Lannuzel, D., and Moreau, S. 2020. "Calving Event Led to Changes in Phytoplankton Bloom Phenology in the Mertz Polynya, Antarctica." Journal of Geophysical Research: Oceans 125 (11). https://doi.org/10.1029/2020JC016387.

Lynn, R. J., and Reid, J. L. 1968. "Characteristics and Circulation of Deep and Abyssal Waters." Deep Sea Research and Oceanographic Abstracts 15 (5): 577–98. https://doi.org/10.1016/0011-7471(68)90064-8.

Measures, C.I., Brown, M.T., Selph, K.E., Apprill, A., Zhou, M., Hatta, M., and Hiscock, W.T.. 2013. "The Influence of Shelf Processes in Delivering Dissolved Iron to the HNLC Waters of the Drake Passage, Antarctica." Deep Sea Research Part II: Topical Studies in Oceanography 90 (June): 77–88. https://doi.org/10.1016/j.dsr2.2012.11.004.

Middag, R., de Baar, H. J. W., Klunder, M. B., and Laan, P. 2013. "Fluxes of Dissolved Aluminum and Manganese to the Weddell Sea and Indications for Manganese Co-Limitation." Limnology and Oceanography 58 (1): 287–300. https://doi.org/10.4319/lo.2013.58.1.0287.

Middag, R., de Baar, H.J.W., Laan, P., Cai, P.H., and van Ooijen, J.C.. 2011. "Dissolved Manganese in the Atlantic Sector of the Southern Ocean." Deep Sea Research Part II: Topical Studies in Oceanography 58 (25–26): 2661–77. https://doi.org/10.1016/j.dsr2.2010.10.043.

Morgan, J. J. 2005. "Kinetics of Reaction between O2 and Mn(II) Species in Aqueous Solutions." Geochimica et Cosmochimica Acta 69 (1): 35–48. https://doi.org/10.1016/j.gca.2004.06.013.

Morton, P. L., Landing, W. M., Shiller, A. M., Moody, A., Kelly, T. D., Bizimis, M., Donat, J. R., De Carlo, E. H., and Shacat, J. 2019. "Shelf Inputs and Lateral Transport of Mn, Co, and Ce in the Western North Pacific Ocean." Frontiers in Marine Science 6 (September): 591. https://doi.org/10.3389/fmars.2019.00591.

Oldham, V. E., Chmiel, R., Hansel, C. M., DiTullio, G. R., Rao, D., and Saito, M. 2021. "Inhibited Manganese Oxide Formation Hinders Cobalt Scavenging in the Ross Sea." Global Biogeochemical Cycles 35 (5). https://doi.org/10.1029/2020GB006706.

Oldham, V. E., Mucci, A., Tebo, B. M., and Luther, G. W. 2017. "Soluble Mn(III)–L Complexes Are Abundant in Oxygenated Waters and Stabilized by Humic Ligands." Geochimica et Cosmochimica Acta 199 (February): 238–46. https://doi.org/10.1016/j.gca.2016.11.043.

Orsi, A. H., Whitworth, T., and Nowlin, W. D. 1995. "On the Meridional Extent and Fronts of the Antarctic Circumpolar Current." Deep Sea Research Part I: Oceanographic Research Papers 42 (5): 641–73. https://doi.org/10.1016/0967-0637(95)00021-W.

Orsi, A. H., and Wiederwohl, C. L. 2009. "A Recount of Ross Sea Waters." Deep Sea Research Part II: Topical Studies in Oceanography 56 (13–14): 778–95. https://doi.org/10.1016/j.dsr2.2008.10.033.

Pardo, C. P., Tilbrook, B., Langlais, C., Trull, T. W., and Rintoul, S. R. 2017. "Carbon Uptake and Biogeochemical Change in the Southern Ocean, South of Tasmania." Biogeosciences 14 (22): 5217–37. https://doi.org/10.5194/bg-14-5217-2017.

Patel, R. S., Llort, J., Strutton, P. G., Phillips, H. E., Moreau, S., Conde Pardo, P., and Lenton, A. 2020. "The Biogeochemical Structure of Southern Ocean Mesoscale Eddies." Journal of Geophysical Research: Oceans 125 (8). https://doi.org/10.1029/2020JC016115.

Peers, G., and Price, N. M. 2004. "A Role for Manganese in Superoxide Dismutases and Growth of Iron-Deficient Diatoms." Limnology and Oceanography 49 (5): 1774–83. https://doi.org/10.4319/lo.2004.49.5.1774.

Rees, C., Pender, L., Sherrin, K., Schwanger, C., Hughes, P., Tibben, S., Marouchos, A. and Rayner, M. 2018. Methods for reproducible shipboard SFA nutrient measurement using RMNS and automated data processing. Limnology and Oceanography: Methods, vol. 17, no 1, p. 25-41. doi:10.1002/lom3.10294

Resing, J. A., Sedwick, P. N, German, C. R., Jenkins, W. J., Moffett, J. W., Sohst, B. M. and Tagliabue, A. 2015. Basin-scale transport of hydrothermal dissolved metals across the South Pacific Ocean. Nature 523, 200–203 (2015). https://doi.org/10.1038/nature14577

Rintoul, S. R. 1998. "On the Origin and Influence of Adélie Land Bottom Water." In Antarctic Research Series, edited by Stanley S. Jacobs and Ray F. Weiss, 151–71. Washington, D. C.: American Geophysical Union. https://doi.org/10.1029/AR075p0151.

Sherrell, R. M., Annett, A. L., Fitzsimmons, J. N., Roccanova, V. J., and Meredith, M. P. 2018. "A 'Shallow Bathtub Ring' of Local Sedimentary Iron Input Maintains the Palmer Deep Biological Hotspot on the West Antarctic Peninsula Shelf." Philosophical Transactions of

715 the Royal Society A: Mathematical, Physical and Engineering Sciences 376 (2122):
716 20170171. https://doi.org/10.1098/rsta.2017.0171.

717 Silvano, A., Rintoul, S. R., Peña-Molino, B., and Williams, G. D. 2017. "Distribution of Water
718 Masses and Meltwater on the Continental Shelf near the Totten and Moscow University
719 Ice Shelves." Journal of Geophysical Research: Oceans 122 (3): 2050–68.
720 https://doi.org/10.1002/2016JC012115.

721 Smith, A. J. R., Ratnarajah, L., Holmes, T. M., Wuttig, K., Townsend A. T., Westwood, K., Cox
722 M., Bell, E., Nicol, S., and Lannuzel, D. 2021. "Circumpolar Deep Water and Shelf
723 Sediments Support Late Summer Microbial Iron Remineralization." Global
724 Biogeochemical Cycles 35 (11). https://doi.org/10.1029/2020GB006921.

725 Snow, K., Sloyan, B. M., Rintoul, S. R., Hogg, A. McC., and Downes, S. M.. 2016. "Controls on
726 Circulation, Cross-shelf Exchange, and Dense Water Formation in an Antarctic Polynya."
727 Geophysical Research Letters 43 (13): 7089–96. https://doi.org/10.1002/2016GL069479.

728 Spreen, G., Kaleschke L. and Heygster, G. 2008. Sea ice remote sensing using AMSR-E 89-GHz
729 channels. Journal of Geophysical Research: Oceans, 113(C2).
730 doi:10.1029/2005JC003384.

731 Sunda, W. G., and Huntsman, S. A. 1988. "Effect of Sunlight on Redox Cycles of Manganese in
732 the Southwestern Sargasso Sea." Deep Sea Research Part A. Oceanographic Research
733 Papers 35 (8): 1297–1317. https://doi.org/10.1016/0198-0149(88)90084-2.

734 ———. 1994. "Photoreduction of Manganese Oxides in Seawater." Marine Chemistry 46 (1–2):
735 133–52. https://doi.org/10.1016/0304-4203(94)90051-5.

736 Sundby, B., Anderson, L. G., and Hall, J.. 1986. "The Effect of Oxygen on Release and Uptake
737 of Cobalt, Manganese, Iron and Phosphate at the Sediment-Water Interface," 8.

738 Tonkin, J. W., Balistrieri, L. S., and Murray, J. W. 2004. "Modeling Sorption of Divalent Metal
739 Cations on Hydrous Manganese Oxide Using the Diffuse Double Layer Model." Applied
740 Geochemistry 19 (1): 29–53. https://doi.org/10.1016/S0883-2927(03)00115-X.

741 Twining, B. S., Baines, S. B., Fisher, N. S and Landry M. R. 2004. Cellular iron contents of
742 plankton during the Southern Ocean Iron Experiment (SOFeX). Deep Sea Research Part
743 I: Oceanographic Research Papers, 2004, vol. 51, no 12, p. 1827-1850.

744 Twining, B. S., Rauschenberg, S., Morton, P. L., and Vogt, S. 2015. "Metal Contents of
745 Phytoplankton and Labile Particulate Material in the North Atlantic Ocean." Progress in
746 Oceanography 137 (September): 261–83. https://doi.org/10.1016/j.pocean.2015.07.001.

747 van der Merwe, P., Wuttig, K., Holmes, T., Trull, T. W., Chase, Z., Townsend, A. T., Goemann,
748 K. and Bowie, A. R. 2019. "High Lability Fe Particles Sourced From Glacial Erosion
749 Can Meet Previously Unaccounted Biological Demand: Heard Island, Southern Ocean."
750 Frontiers in Marine Science 6 (June): 332. https://doi.org/10.3389/fmars.2019.00332.

751 Wagener, T., Guieu, C., Losno, R., Bonnet, S., and Mahowald, N. 2008. "Revisiting
752 Atmospheric Dust Export to the Southern Hemisphere Ocean: Biogeochemical
753 Implications." Global Biogeochemical Cycles 22 (2): n/a-n/a.
754 https://doi.org/10.1029/2007GB002984.

755 Wedepohl, K Hans. 1995. "The Composition of the Continental Crust," 16.

Westerlund, S., and Öhman, P. 1991. "Iron in the Water Column of the Weddell Sea." Marine Chemistry 35 (1–4): 199–217. https://doi.org/10.1016/S0304-4203(09)90018-4.

Whitworth, T., Orsi, A. H., Kim, S.J., Nowlin, W. D., and Locarnini, R. A. 1985. "Water Masses and Mixing Near the Antarctic Slope Front." In Antarctic Research Series, edited by Stanley S. Jacobs and Ray F. Weiss, 1–27. Washington, D. C.: American Geophysical Union. https://doi.org/10.1029/AR075p0001.

Wu, M., Scott, J., McCain, P., Rowland, E., Middag, R., Mats, S., Allen, A. E., and Bertrand, E. M. 2019. "Manganese and Iron Deficiency in Southern Ocean Phaeocystis Antarctica Populations Revealed through Taxon-Specific Protein Indicators." Nature Communications 10 (1): 3582. https://doi.org/10.1038/s41467-019-11426-z.

Wuttig, K., Townsend, A. T., van der Merwe, P., Gault-Ringold, M., Holmes, T., Schallenberg, C., Latour, P. et al. 2019. "Critical Evaluation of a SeaFAST System for the Analysis of Trace Metals in Marine Samples." Talanta 197 (May): 653–68. https://doi.org/10.1016/j.talanta.2019.01.047.

Xu, G., and Gao, Y. 2014. "Atmospheric Trace Elements in Aerosols Observed over the Southern Ocean and Coastal East Antarctica." Polar Research 33 (1): 23973. https://doi.org/10.3402/polar.v33.23973.